RSC Sustainability

ROYAL SOCIETY OF CHEMISTRY

PAPER

View Article Online
View Journal | View Issue

Cite this: *RSC Sustainability*, 2025, **3**, 599

Preparation of marine-sourced alginate fibres to produce composite paper from both green and blue carbons

RM. Muhammad Nur Fauzan,[a] Kotchaporn Thangunpai,[a] Akiko Nakagawa-Izumi,[b] Mikio Kajiyama[b] and Toshiharu Enomae *[b]

Recent trends in papermaking have led to an increase in the use of alternative resources. Alginate fibres, derived from marine sourced brown seaweed (blue carbon), offer a potential alternative to wood pulp in paper production. The process of obtaining alginate involves pre-treatment, alkaline extraction, precipitation, and purification. Through successful extraction, alginates were obtained from *Laminaria japonica* (*L. japonica*) and *Sargassum polycystum* (*S. polycystum*) with yields ranging from 17.4% to 28.9% and 14.7% to 26.8%, respectively. The molecular mass of the alginates ranged from 0.68×10^5 to 2.74×10^5 g mol^{-1} for *L. japonica* and from 0.39×10^5 to 0.994×10^5 g mol^{-1} for *S. polycystum*. Calcium alginate fibres and wood pulp fibres were combined to create composites. The results from this study suggest that the composites achieved an optimum tensile index when the samples contained 50% calcium alginate fibres. Although the results were promising, the tensile index of the paper made exclusively from pulp fibres remained superior. Furthermore, thermal degradation tests demonstrated improved thermal stability for the composite papers compared to hardwood bleached kraft pulp (HBKP) sheets. In conclusion, a composite prepared from a mixture of calcium alginate and wood pulp fibres was successfully produced and overall 50% inclusion of calcium alginate fibres provided an optimum composite.

Received 14th February 2024
Accepted 13th November 2024

DOI: 10.1039/d4su00073k

rsc.li/rscsus

Sustainability spotlight

Global warming caused by the emission of carbon dioxide gas and the greenhouse effect (GHG) is the most serious, pressing environmental problem facing people around the world today. To efficiently restrain the emission of carbon dioxide gas (CO_2) into the atmosphere, forestation is an efficient way to solidify it as green carbon; however, the land area for green carbon storage is planar and limited, while the capacity of carbon storage of oceans is huge, considering that there are many varieties of aquatic organisms from shallow waters to the deep sea. The oceans are home to a wide variety of aquatic organisms called blue carbon. Then, there is much larger accumulation of carbon in the ocean than on land; therefore, circular utilization of blue carbon in a larger amount is sustainable and more advantageous than green carbon; therefore, the subject of this study focuses on the utilization of brown seaweed as blue carbon.

1. Introduction

Since their invention, plastics have become an important material in our daily lives. However, decades of accumulation of plastic have resulted in significant environmental problems due to their innumerable uses. More than 10 million tons of plastic waste end up in the oceans annually and more than 80% of the marine litter is plastic.[1] Some plastic wastes, such as disposable plastic containers and plastic bags, end up in the marine environment, leading to the accumulation of microplastics that are further subdivided and float. Additionally, a pressing issue is global warming which is exacerbated by increasing CO_2 emissions coming from plastic production. Such problems not only disrupt food chains and aquatic ecosystems, but also contribute to global warming. Therefore, the replacement of petroleum-based plastics with biodegradable plastic and paper needs to be accelerated.

Advanced biomaterial-based innovations seem to ensure sustainability and address waste disposal problems. However, raw bio-based materials, such as polysaccharides and proteins, are mainly harvested from agricultural plants, which may pose a potential threat to the stability of the food supply.[2] Currently, seaweeds and microalgae are gaining increasing attention as promising potential resources because of their high growth rate and extensive environmental tolerance, significantly alleviating the competition between food and water resources.[3,4] An alginate is a polysaccharide that exists mostly in the cellular wall

[a]*Degree Programs in Life and Earth Sciences, University of Tsukuba, Tsukuba, Ibaraki, 305-8572, Japan. E-mail: enomae.toshiharu.fw@u.tsukuba.ac.jp*
[b]*Institute of Life and Environmental Sciences, University of Tsukuba, Tsukuba, Ibaraki, 305-8572, Japan*

matrix of brown seaweeds and can be extracted from them. The sequence of the saccharide units consists of β-(1 → 4)-D-mannuronic (M) and α-L-guluronic acid (G) blocks in varying proportions. Alginates are responsible for the springiness and mechanical strength required by seaweeds to survive in the ocean.[5] Alginates are widely used in various industrial sectors, including the food, textile, medical, and pharmaceutical industries.[6] In addition, the flame-retardant properties typical of alginates can open up a wide range of potential applications, including firefighters and military apparel, domestic furnishings like padding, interior fittings such as thermal and sound insulation for walls, and structural coatings for wooden beams.[7] Despite these potential benefits, the literature on the flame retardancy of alginates remains relatively limited, as most research has focused on their biomedical applications.[7]

Research on alginates and other polysaccharides has increased over the past decade due to growing awareness of the need for sustainable materials to replace fossil resource-based products.[8] Alginate can be cross-linked to form a hydrogel in the presence of divalent ions such as Ca^{2+}. Based on the ability to form gels with metal ions, various alginate-based materials with different morphologies have been developed, such as alginate hydrogel beads,[9,10] alginate fibers,[11,12] and so on.

In Indonesia, *S. polycystum* is classified as a brown seaweed that is widely distributed. However, its utilization remains low and it has a low market value in Indonesia.[13] On the other hand, in Japan, one of the popular seaweed products is the sea kelp known as *Kombu*. These kelps are large seaweeds that belong to the *L. japonica* species of brown seaweed. Kombu is often used in flavoured dishes, soup stocks, boiled vegetables, snacks, or seasoning for rice.[14] It is also used for other dishes such as *Kombu tsukudani*, *Kombu* dressing, or *Kombu* chips, and finally for feedstuff or non-edible use as a material. Both *S. polycystum* and *L. japonica* are categorized as brown seaweeds with a high alginate content.

The first step in extracting alginate from seaweed involves drying the seaweed. The dried seaweed is then cut into small pieces. Size reduction of dried seaweed promotes extraction efficiency because smaller particles have a higher surface area, leading to an increase in contact with the solvents during the pre-treatment or extraction stages.[5] For the pre-treatment process, Andriamanantoanina and Rinaudo[15] bleached *Sargassum* sp. with sodium hypochlorite (NaOCl) and obtained white alginates because the bleaching process removes the colour pigments present in *Sargassum* sp. Acid pretreatment is usually conducted before alkaline extraction. In brown seaweeds, alginic acid is mainly present as a calcium salt although potassium, magnesium, and sodium salts may also be present.[16] After conversion to alginate acid during acid pretreatment, insoluble alginic acid is formed and possibly converted into a soluble form, such as sodium alginate by reacting it with sodium carbonate. Subsequently, a crude sodium alginate solution was obtained.

There are two methods for producing alginate after brown seaweed is extracted. One method is calcium chloride addition, by which precipitation is carried out with a calcium chloride solution to obtain calcium alginate as a precipitate. The other method is acid addition, by which a strong acid solution is used to obtain an alginic acid gel.[17] In both methods, the separated solid form of alginate is commonly converted to a sodium alginate solution by reacting with sodium carbonate and subsequently precipitated with an organic solvent such as ethanol.[18]

One of the most remarkable properties of alginates is their ability to form gels through coordination with divalent cations (*e.g.*, Ca^{2+}, Sr^{2+}, and Ba^{2+}) or trivalent cations (*e.g.*, Al^{3+} and Fe^{3+}) that enables their vast industrial utilization in turn. This mechanism, commonly known as the egg-box model, describes in general two antiparallel alginate chains that form polyelectrolyte complexes (PECs) by electrostatically interacting with positively charged ions through their negatively charged carboxyl groups.[19]

A common, simple way to fabricate alginate-based materials is wet spinning to form a fibre-like shape and adding dropwise an alginate solution into a calcium chloride bath to obtain cross-linked beads. Another fibre-forming technique, including electrospinning, has demonstrated considerable potential in biomedical fields such as tissue engineering, wound healing, and drug delivery. The use of electrospun alginates and other naturally derived biopolymers to create scaffolds has the potential to exploit an area of active and promising research.[19,20] Kobayashi *et al.*[11] produced alginate fibres and made a paper sheet from them and mentioned that paper sheets were successfully formed from alginate fibres without any binder. This discovery is interesting because there was also a papermaking trend shifting to the use of non-wood fibre materials.

In this study, brown algae consisting of alginate fibres from *S. polycystum* and *L. japonica* were used as substitutional fibre sources to complement wood pulp fibres to produce composite paper. Previous research has extensively covered the use of wood pulp in paper production and the properties of alginate fibres in various applications. However, studies on the integration of calcium alginate fibres with wood pulp for composite paper production are among the few cases. The resulting composite paper can enhance properties, improve biodegradability, and reduce environmental impact differently compared to conventional plastic-based materials. This research aims to explore the preparation and characterization of composite paper from marine-sourced (blue carbon) alginate fibres and wood pulp fibres (green carbon) to find out whether paper composites can serve as a viable alternative to plastics in various applications, including packaging.

By using alginate fibres as a component of the composites, the optimum conditions were pursued to improve its properties, which were determined using scanning electron microscopy (SEM), tensile strength, thermogravimetric analysis (TG), X-ray diffraction analysis (XRD), and X-ray photoelectron spectroscopy (XPS) as well as mechanical strength tests.

2. Materials and methods

2.1 Materials

Dried brown seaweed (*S. polycystum*) and dried *Kombu* (*L. japonica*) were purchased from markets in East Java, Indonesia,

and Japan, respectively. Hardwood bleached kraft pulp (HBKP), sodium hypochlorite (NaOCl), sulfuric acid (H_2SO_4), sodium carbonate (Na_2CO_3), calcium chloride ($CaCl_2$), and ethanol were purchased from Fujifilm Wako Pure Chemical (Osaka, Japan). Deionized water (DW) used for the entire experiment was obtained from a WR600G ultraviolet water purification system (Yamato Scientific, Tokyo, Japan).

2.2 Bleaching treatment of the brown seaweeds

10 g of dried seaweed was bleached with a NaOCl solution containing 3% active chlorine obtained by diluting 5% commercial active chlorine (Fujifilm Wako Pure Chemical Corporation, Japan) for 10 min to eliminate the pigments. The bleached seaweeds were then rinsed until the pH was almost neutral.

2.3 Extraction process with sodium alginate

The bleached seaweed and unbleached seaweed were first immersed in 200 mL of 0.05 M H_2SO_4 at 40 °C for 1 h, sieved, washed until the pH was almost neutral, and centrifuged, so that they can be separated easily from the washing water. Subsequently, the acid-treated seaweed was reacted with 200 mL of 2% Na_2CO_3 solution at 70 °C for 2 h. Then, filtration was carried out through a muslin cloth to remove agglomerates and centrifuged. Finally, the crude sodium alginate solution was obtained. The samples processed *via* the bleaching process are referred to as Bleached Sargassum (BS) and Bleached Kelp (BK), while the samples not subjected to the bleaching process are referred to as Unbleached Sargassum (US) and Unbleached Kelp (UK).

2.4 Purification and precipitation process of sodium alginate

Two different purification processes were used, and the calcium and acid routes were compared with the crude sodium alginate solution obtained in Fig. 1. The precipitation process followed the method described by Gomez *et al.*[21] with some modifications.

2.4.1. Acid route. In this route, the crude sodium alginate solution was mixed with 200 mL of 0.5 M H_2SO_4 using a magnetic stirrer at room temperature (RT) for 1 h (pH 2). Next, the alginic acid gel was washed and separated *via* centrifugation. The alginic acid gel was added to 200 mL of 0.5 M Na_2CO_3 and mixed using a magnetic stirrer at RT for 1 h to convert it to sodium alginate. The solution was then precipitated by the addition of ethanol (1 : 1 volume ratio), centrifuged, and dried at 40 °C.

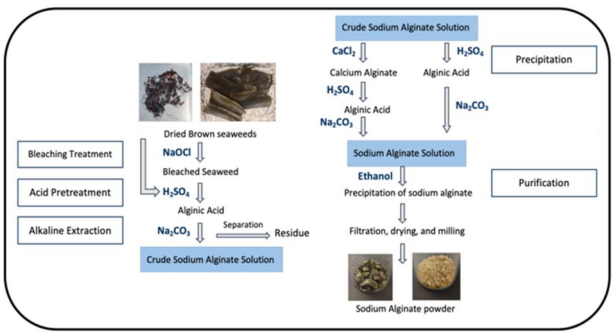

Fig. 1 Schematic diagram for the extraction of sodium alginates.

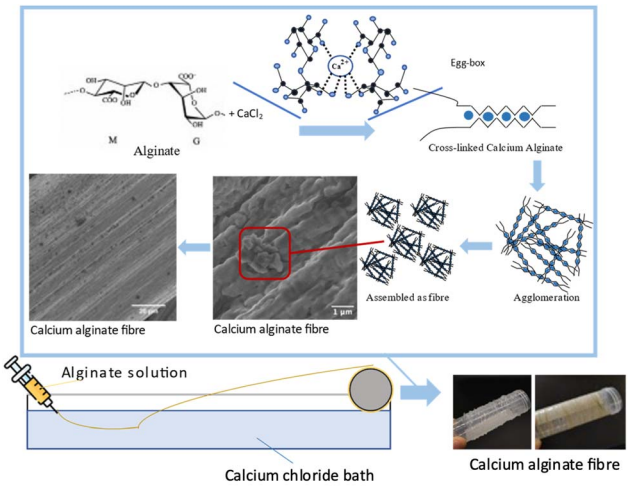

Fig. 2 Mechanisms involved in the production of alginate fibres by a chemical reaction between sodium alginate and calcium chloride with SEM images of calcium alginate fibres surfaces with its spinning process.

2.4.2 Calcium route. The crude sodium alginate solution was precipitated by the addition of 200 mL of 0.5 M $CaCl_2$ solution. Calcium alginate was washed with DW and filtered. Then, 200 mL of 0.5 M H_2SO_4 was added and stirred at RT for 2 h. The alginic acid was washed and separated by centrifugation and 200 mL of 0.5 M Na_2CO_3 was added and mixed using a magnetic stirrer at RT for 2 h to convert it to sodium alginate by ion exchange. The solution was precipitated by addition of ethanol (1 : 1 volume ratio), centrifuged, and dried at 40 °C. The samples produced through the acid route process are referred to as the Bleached Sargassum Acid Route (BSAR), Bleached Kelp Acid Route (BKAR), Unbleached Sargassum Acid Route (USAR) and Unbleached Kelp Acid Route (UKAR). While the samples that undergo the calcium route process are referred to as the Bleached Sargassum Calcium Route (BSCR), Bleached Kelp Calcium Route (BKCR), Unbleached Sargassum Calcium Route (USCR), and Unbleached Kelp Calcium Route (UKCR).

2.5 Calcium alginate fibre production through the wet spinning process

A 3% sodium alginate solution was syringed with a 28-gauge needle and then extruded into a 5% $CaCl_2$ solution bath. The extruded solution became fibrous, and it was dried at RT. The reproduced calcium alginate fibres were cut into short fibres approx. 2 mm long. Fig. 2 shows the chemical reaction between sodium alginate and the calcium chloride solution. In this process, three types of calcium alginate fibres were prepared, namely, a commercial alginate fibres (CA), kelp calcium alginate fibres (KA), and sargassum calcium alginate fibres (SA). CA

Table 1 Paper composite formulation[a]

No	Sample name	Wood pulp fibres (%)	CA fibres (%)	KA fibres (%)
1	HBKP	100	0	0
2	CA25	75	25	0
3	CA50	50	50	0
4	CA75	25	75	0
5	KA25	75	0	25
6	KA50	50	0	50
7	KA75	25	0	75

[a] CA: commercial alginate and KA: kelp alginate.

was prepared in the spinning process from commercially available sodium alginates fabricated into fibres for comparison. In contrast, seaweed calcium alginate fibres and sargassum calcium alginate fibres were both alginate samples obtained from previous samples and fabricated into fibres.

2.6 Preparation of laboratory sheets

Wood pulp fibres and calcium alginate fibres were used in the formation of laboratory sheets. A total of 27 g of dry HBKP was weighed and immersed in water for 1 day. Then, the wet pulp was dispersed well with a disintegrator for 5 min. The disintegrated pulp was sieved, collected, and subjected to beating to enhance the mechanical strength of the laboratory sheets, by swelling and increasing the flexibility of fibres. In the beating process, pulp was put into a mill house of a PFI mill and rotated 5000 times. Subsequently, 7.8 L water was then added to the beaten pulp, and the pulp was dispersed well with a mixer in a bucket. Consequently, a final pulp concentration of 0.15% was reached, and then 800 mL of pulp suspension was taken per sheet. To obtain a composite of paper, we designed the experiment by adding calcium alginate fibres, as shown in Table 1. The wet sheets were dried at RT for 24 h. Finally, the laboratory sheets were prepared for further evaluation.

2.7 Capillary viscometry: viscosity and molecular weight

The kinematic viscosity (ν) was determined using a Cannon-Fenske routine viscometer with a 0.1 M NaCl aqueous solution as a solvent. For each sample, five measurements were made at 25 °C ± 0.1 °C according to Torres *et al.*[22] Alginate solutions (30 g L^{-1}) were prepared by stirring at RT for 4 h. After measuring the absolute viscosity of the solvent (η_0) and alginate solutions (η_s), the relative viscosity (η_r) and specific viscosity (η_{sp}) were calculated according to eqn (1) and (2):

$$\eta_r = \eta_s/\eta_0 \quad (1)$$

$$\eta_{sp} = \eta_r - 1 \quad (2)$$

The intrinsic viscosity is a measure of the hydrodynamic volume occupied by the macromolecule at infinite dilution in a specific solvent at a given temperature and is defined by the Huggins equation (eqn (3)) as follows:

$$[\eta] = \lim_{c\to 0} \eta_{sp}/c \quad (3)$$

The intrinsic viscosity was determined in dilute solutions using eqn (4), where η_{sp}/c is the reduced viscosity and k_h is the Huggins constant.

$$\eta_{sp}/c = [\eta] + k_h [\eta]^2 c \quad (4)$$

Then, the obtained intrinsic viscosity was used to estimate the molecular weight of alginate using the Mark–Houwink equation (eqn (5)), as follows:

$$[\eta] = K M_v^{\alpha} \quad (5)$$

K and α values depend on the polymer and solvent-temperature systems. The study by Clementi *et al.*[23] proposed empirical relationships for $[\eta]$ and the average molecular weight (M_w) so the eqn (6) becomes:

$$[\eta] = 0.023 M_v^{\alpha 0.984}, \quad (6)$$

where $[\eta]$ is the intrinsic viscosity given in dL g^{-1} and M in kilodaltons. The M_w values for alginates from *L. japonica* and *S. polycystum* were estimated from the intrinsic viscosity data.

2.8 Analysis of functional properties by Fourier transform infrared spectroscopy (FTIR)

FTIR spectra of sodium alginate and paper sheet composites were recorded using a FTIR spectrometer (FT/IR-6100, JASCO Corporation, Japan) combined with an ATR (PRO ONE PKS-Z1, JASCO Corporation, Japan) spectrometer with a Ge prism (PKS-G1, JASCO Corporation, Japan) as a reference in the range of 500–4000 cm^{-1} to examine the possible changes in functional groups induced by various treatments.

2.9 Analysis of surface morphology by field emission scanning electron microscopy (FESEM)

The surface morphologies of the calcium alginate fibres and paper composites were analysed using FESEM (SU8020, Hitachi, Japan) with an accelerating voltage of 5 kV. All samples were coated with platinum (Pt) through sputtering for electroconductivity before observation.

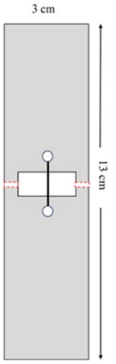

Fig. 3 A paper frame used for gluing a single fibre specimen.

2.10 Tensile strength of single fibres

The tensile strength of single calcium alginate fibres was measured in accordance with a modification of the preparation procedure described in ASTM D3822-07. Mechanical tests were conducted using a tensile and compression tester (MCT-2150, A&D Company, Japan) at a crosshead speed of 10 mm min^{-1}.

Each fibre specimen with a length of approximately 20 mm was glued to the paper frame. Both ends of a fibre were glued with an adhesive to the paper frame, as shown in Fig. 3. Upon clamping the ends of the supporting frame using the jaws of the tensile testing machine, the frame edges were carefully cut at the centre. The tensile parameters were determined when the fibres broke immediately after the maximum elongation. In this experiment, 25 fibre samples were prepared to obtain the average data.

2.11 Tensile strength of the paper composites

The tensile strength of the paper composites was measured using ISO standard 5270. Mechanical tests were conducted using a tensile and compression tester (MCT-2150, A&D Company, Japan) installed under environmental conditions of 23 °C and 50% RH with a crosshead speed of 10 mm min^{-1} and a clamping span of the specimens of 100 mm. Each specimen had a width of 15 mm and a length of 130 mm or longer (Fig. 4). The tensile strength was determined and recorded immediately after the paper broke when the maximum elongation was reached.

2.12 Thermal stability based on thermogravimetric analysis (TGA)

The thermal stability of alginate fibres and paper composites was measured using a thermogravimetric analyser (TG/DTA 7300 Exstar, Seiko, Japan). Approximately 5–10 mg samples were heated from 50 to 900 °C at a heating rate of 20 °C min^{-1} under an argon atmosphere at a flow rate of 200 mL min^{-1}.

2.13 Analysis of inorganic particle formation

X-ray diffraction patterns of the composite paper (HBKP, CA (25, 50, 75), and KA (25, 50, 75)) and the samples after the thermal treatment of calcium alginate fibres (CA and KA) thermally treated at 200, 400, 600 and 800 °C were recorded using an XRD (D8 Advance/TSM, AXS-Bruker, Germany) as a function of 2θ ranging from 10° to 60° at 40 kV and 40 mA using a CuK_α (λ = 1.5406 Å) source.

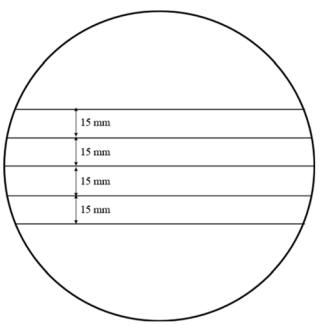

Fig. 4 The preparation of the paper specimen for tensile strength measurement.

2.14 Analysis of chemical composition

The chemical compositions of the samples were analysed using XPS (JPS-9010TR, JEOL, Tokyo, Japan) with an AlK_α radiation (1486.6 eV) source at 10 kV and 20 mA.

3. Results and discussion

3.1 Sodium alginate yield

The yield of sodium alginate is shown in Fig. 5. It shows that the yield of sodium alginate obtained through the calcium route was higher. In general, alginate content in brown seaweeds varies from 20 to 30% of the dried weight of seaweeds.[24] The amount of sodium alginate extracted in this study from *S. polycystum* was 14.4–26.8% and that from *L. japonica* was 17.4–28.9%. Additionally, the amounts of alginate were found to vary from species to species of brown seaweed all over the world from previous studies, such as 16.9% in *S. muticum*,[25] 22.0–33.7% in Madagascan *Sargassum* species,[18] 10.0–33.3% in Indonesian *Sargassum* species,[13] 21.1% in *L. japonica*,[26] and 14.6–29.5% in *L. japonica*.[27] The yield of sodium alginate obtained in this experiment was in the range of general results.[24]

The bleached sodium alginate gave a lower yield than the unbleached one. The yield of sodium alginate in Fig. 5 resulting from the different processes of precipitation between the acid and calcium routes showed that *S. polycystum* and *L. japonica* species were 3.8% (USCR to BSCR), 6.2% (USAR to BSAR), 6.4% (UKCR to BKCR) and 9.1% (UKAR to BKAR). The result also agreed with that of Istini *et al.*,[28] in which the bleaching process reduced the yield of sodium alginates obtained due to the possible oxidation and material loss during the process.

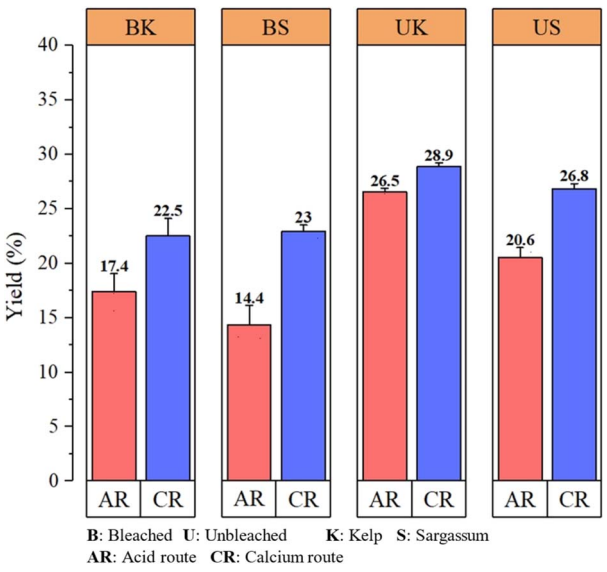

Fig. 5 Yield of sodium alginate from *S. polycystum* and *L. japonica*.

Table 2 Intrinsic viscosity and average molecular weight estimation of sodium alginate samples

No	Brown seaweed species	Sample name	Intrinsic viscosity [η] (L g^{-1})	$M_w^{\alpha} \times 10^5$ (g mol^{-1})	R^2
1	*S.polycystum*	BSAR	0.14	0.63	0.956
2		BSCR	0.07	0.34	0.984
3		USAR	0.21	0.99	0.912
4		USCR	0.18	0.84	0.909
5	*L. japonica*	BKAR	0.17	0.79	0.936
6		BKCR	0.15	0.68	0.970
7		UKAR	0.58	2.74	0.996
8		UKCR	0.38	1.89	0.954
9	Commercial alginate	CMAL	0.55	2.60	0.960

Additionally, the purification process was found to be one of the factors for the low yield of sodium alginates. Fig. 5 shows that the yield *via* the calcium route was higher than that *via* the acid route because calcium ions have a strong affinity for alginate molecules, leading to strong bonds between sodium alginates and calcium ions. In contrast, the acid route *via* the addition of an acid, such as sulfuric acid, may cause some degradation of alginate molecules, resulting in a lower yield of sodium alginates. This finding was confirmed by Lim *et al.*[29] The yield of sodium alginates from *Sargassum* sp. was higher *via* the calcium route than the acid route.

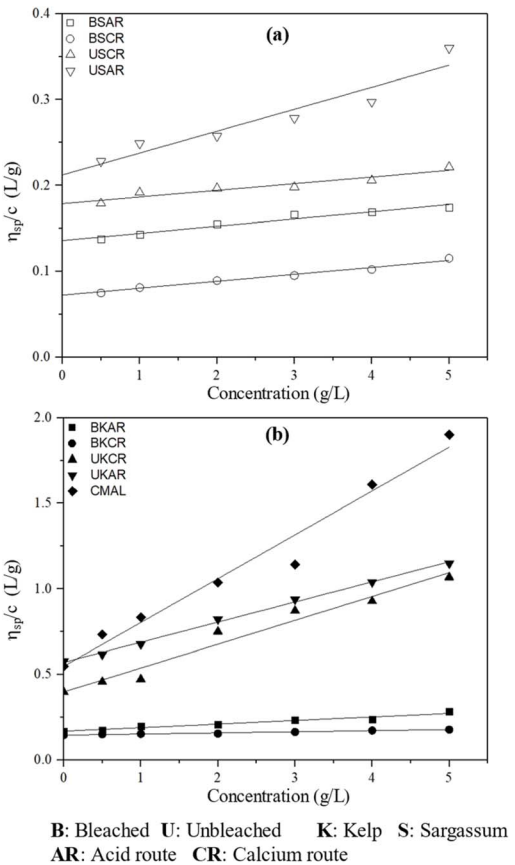

Fig. 6 Specific viscosity (η_{sp}) of sodium alginate samples in 0.1 M NaCl from (a) *S. polycystum* and (b) *L. japonica*.

3.2 Sodium alginate characterization

3.2.1 Intrinsic viscosity ([η]) and molecular weight (M_w^{α}).

The intrinsic viscosity and molecular weight based on the molar mass of sodium alginates from *S. polycystum* are shown in Table 2 and Fig. 6, ranging from 0.07 to 0.21 L g^{-1} and 0.338 to 0.994 $\times$ 10^5 g mol^{-1}, and the molar mass of sodium alginates from *L. japonica* ranged from 0.15 to 0.58 dL g^{-1} and 0.679 to 2.74 $\times$ 10^5 g mol^{-1}, and for commercial sodium alginates (CMAL) it was 0.55 L g^{-1}.

This result also demonstrates a regression coefficient (R^2) greater than 0.9, as shown in Table 2, indicating the accuracy of the outcomes.

S. polycystum subjected to various ozonation treatments (bleaching treatment) had intrinsic viscosities ranging from 0.042 to 0.158 dL g^{-1}.[30] The polymer chain was shortened during the bleaching process because of the glycosidic bond breakage. The results show that the intrinsic viscosity of sodium alginates from the bleaching process significantly decreased due to the bleaching treatment. This led to a decrease in molecular weight.[25,30]

The acid route can promote more complete precipitation of sodium alginates, leading to the formation of larger, more

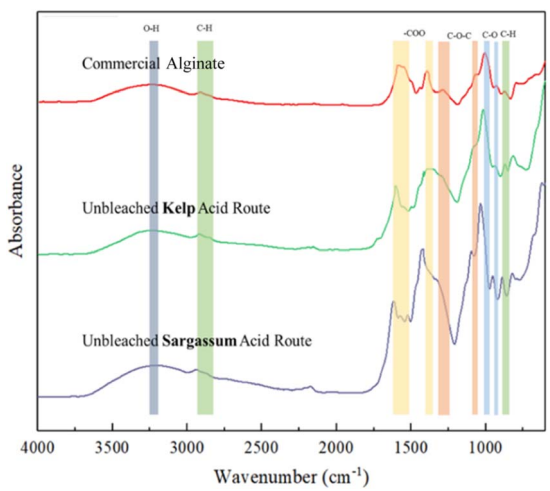

Fig. 7 FTIR of alginate from commercial, *L. japonica*, and *S. polycystum*.

branched aggregates that can increase the viscosity of the solution. However, the calcium route led to lower viscosity owing to the presence of residual calcium ions in the final product. These calcium ions can interfere with the alginate chains, resulting in lower viscosity. These mechanisms were also confirmed by Gomez *et al.*,[21] as they reported that the acid route produced sodium alginates with a higher viscosity than those *via* the calcium route. This could be explained by the breakage of the ether bond by the acid solution used in both the calcium alginate and alginic acid routes, leading to low viscosities. Thus, USAR, UKAR, and CMAL were chosen for further experiments to produce fibres because of their higher molecular weights.

3.2.2 FTIR. Fig. 7 shows the main functional groups and chemical bonds of the commercial alginate and alginates extracted from *S. polycystum* and *L. japonica* as revealed by the FTIR spectra. The commercial alginate and alginates extracted from *S. polycystum*, and *L. japonica* displayed a similar broad absorption peak at 3300 cm^{-1}, which was attributed to OH-bending vibration. In addition, a weak band near 2925 cm^{-1} was attributed to CH-stretching vibration.[31–33] The asymmetric and symmetric stretching vibrations of carboxylate ($R\text{-}COO^{-}$) groups were observed at absorption peaks at approximately 1645 and 1410 cm^{-1}.[31,33] The peak at approximately 1090 cm^{-1} is assigned to symmetrical C–O–C stretching.[34]

Another peak attributed to alginates was located at 1290 cm^{-1} and was assigned to the C–O–C group.[31] Other peaks at 820 and 940 cm^{-1} correspond to C–H bonds from mannuronic acid and uronic acid residues.[35]

The FTIR spectra of sodium alginates obtained from *S. polycystum* and *L. japonica* clarify that they have a chemical structure similar to that of commercial sodium alginate. This was confirmed by successful extraction of the sodium alginates.

3.3 Single-fibres characteristics

3.3.1 Statistical distribution of tensile strength. Weibull analysis, a commonly used statistical technique for analysing the physical behaviour of brittle materials in terms of strength, was predicated based on the idea that the failure due to the most significant fault caused the overall failure of the specimen.[36] The strength of the fibres was found to be statistically distributed because of the different severities of faults along the volume of the fibres. Therefore, the distribution of the fibre strength, σ_f, under tension is generally described using mean values of the standard Weibull modulus.

$$F = 1 - \exp((-\sigma_f)/\sigma_o)m, \quad (7)$$

where F is the failure probability of the fibres and m is the Weibull modulus, that is, the variability of the distribution. σ_0 denotes the characteristic strength. By rearranging and taking the natural logarithm of the variables on both sides of eqn (5), eqn (6) is obtained:

$$\ln(\ln(1/(1 - F))) = m \ln \sigma_f - m \ln \sigma_o \quad (8)$$

Hence, a plot of $X = \ln \sigma_f$ *vs.* $Y = \ln(\ln(1/(1 - F)))$ should be a straight line if the material strength variability is described by the Weibull distribution. F in eqn (5), also known as the probability index, was estimated using the following approximation:

$$F = (n - 0.5)/N, \quad (9)$$

where n is the rank of the n-th number in the ascending ordered strength data point ($n = 1$ corresponds to the smallest and $i = n$ corresponds to the largest) and N is the total number of samples.

The inherent defect distribution along the fibres and the fibre-to-fibre strength variability within a batch of fibres resulting from processing variances and damage brought about by handling the fibres are two major factors influencing the strength variability. To analyse the statistical distribution of the fibre strength, a plot of the tensile strength for the different sources of calcium alginates based on the Weibull modulus is shown in Fig. 8. In all cases, the R^2 coefficient was relatively high ($\geq$0.95), indicating a satisfactory degree of linearity. Thus, the fibre strength can be effectively described using the Weibull function.

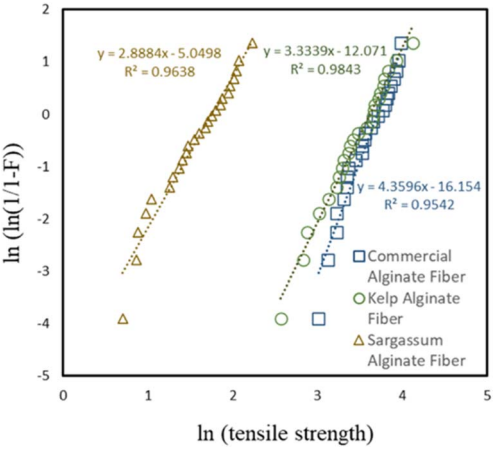

Fig. 8 Weibull plots for different types of calcium alginate fibre sources.

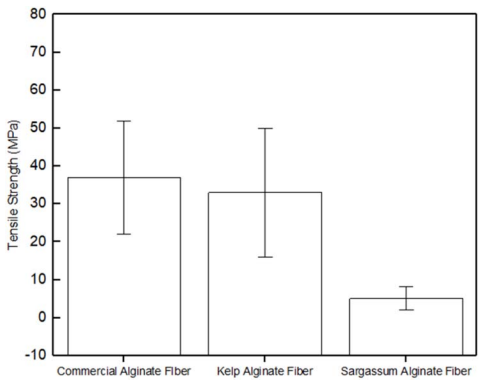

Fig. 9 Tensile strength of calcium alginate fibres from different sources.

3.3.2 Tensile strength of single calcium alginate fibres. The average tensile strengths of a single fibre of commercial alginates, kelp calcium alginates, and *sargassum* calcium alginates are compared in Fig. 9. The results of this study indicate that the tensile strengths of commercial alginate fibres and kelp calcium alginate fibres were higher than that of the *sargassum* calcium alginate fibres.

The lower tensile strength of the *Sargassum* calcium alginate fibres is attributed to the lower viscosity of sodium alginate obtained from *S. polycystum*, as compared to the other two sources. The higher viscosity suggesting a higher molecular weight of the alginate composed of long polysaccharide chains generally leads to stronger fibres.[37] On the other hand, a lower viscosity would result in weak fibres because a low viscosity material is typically more fluid, presumably having an impact on the bonding that occurs during the formation of the fibres. Based on these results, the commercial and kelp calcium alginate fibres were chosen for further experiments.

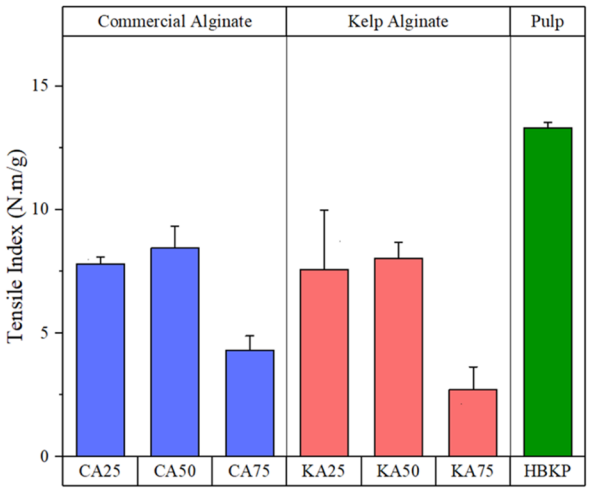

Fig. 11 Tensile index of calcium alginate-containing wood pulp sheets.

3.4 Characterization of paper composites

3.4.1 FESEM. Fig. 10 shows the FESEM images of the morphology of the paper, calcium alginate fibres and paper composites. The calcium alginate fibres (Fig. 10e) display a larger fibre size in comparison to the pulp fibres, as observed in the HBKP sample (Fig. 10a) with the same magnification. While the calcium alginate fibres are bonded, their structure appears weaker compared to the pulp fibres, which are smaller and more uniform.

3.4.2 Tensile index. Fig. 11 shows the tensile index of a paper composite consisting of pulp fibres mixed with and without alginate fibres obtained from *L. japonica* and commercial alginate. The tensile strength results showed that the formulations CA25, KA25, CA50, and KA50 exhibited an improvement in the tensile index compared to CA75 and KA75.

However, the tensile strength with the addition of alginate fibres was still lower than that of the control (paper containing only pulp fibres). This is also confirmed by other studies clarifying that the mechanical strengths of a cotton/alginate composite decreased with increasing alginate content.[38] As can be seen from the fracture, interaction among calcium alginate fibres is not particularly strong, as shown in Fig. 12.

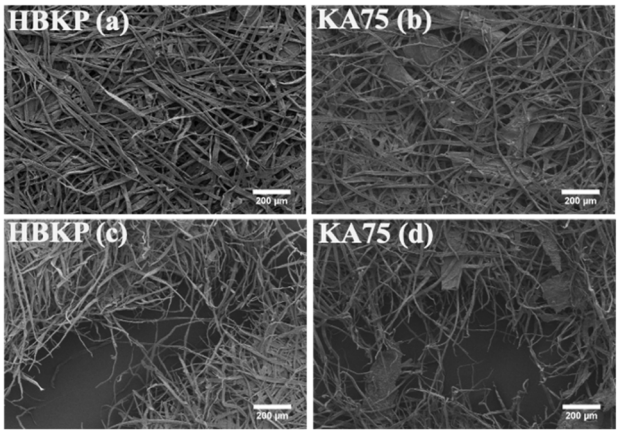

Fig. 12 SEM image before fracture and after fracture of HBKP (a and c) and KA75 (b and d).

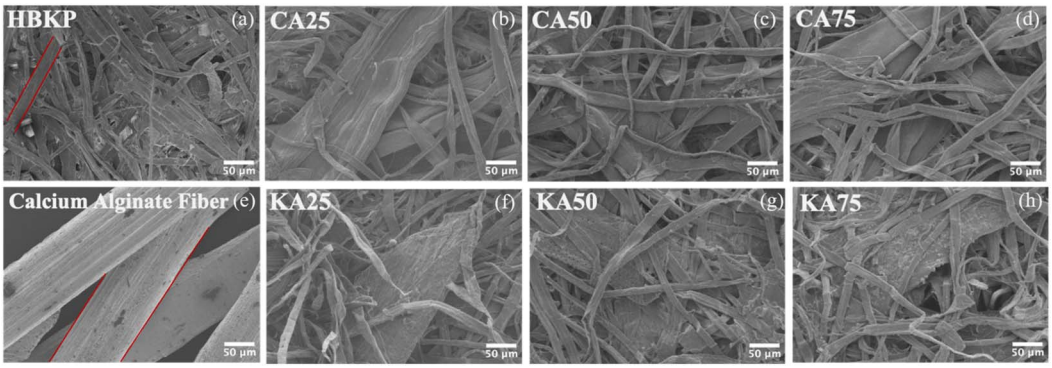

Fig. 10 SEM images of (a) HBKP, paper composites containing commercial alginate (CA) fibres: (b) 25%, (c) 50%, and (d) 75%, (e) calcium alginate fibres, and paper composites containing kelp alginate (KA) fibres: (f) 25%, (g) 50% and (h) 75%.

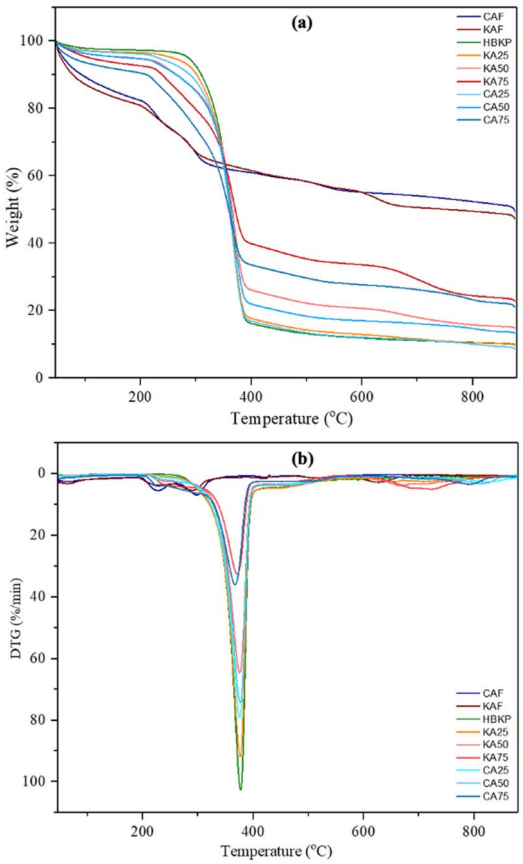

Fig. 13 (a) Thermogravimetric (TG) and (b) DTG curves of calcium alginate fibres and paper composites.

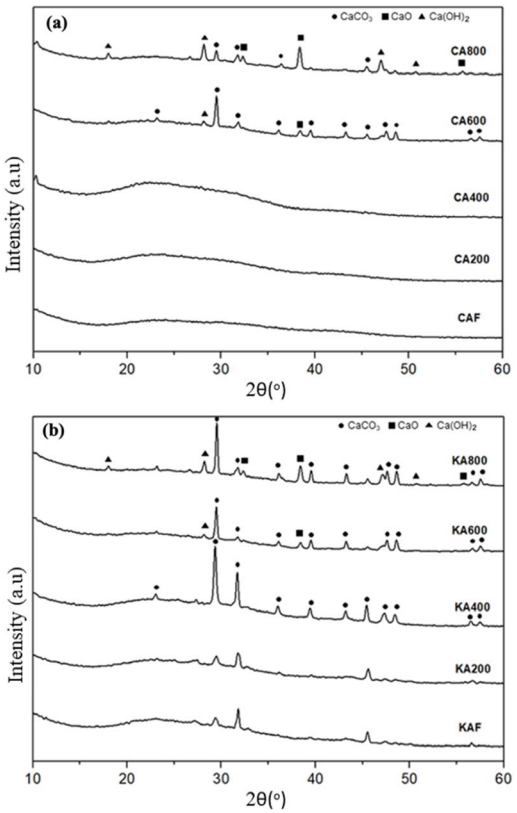

Fig. 14 XRD patterns of the residual calcium alginate from (a) commercial alginate fibres (CA) and (b) kelp alginate fibres (KA) after thermal treatment at 200, 400, 600, and 800 °C.

3.4.3 Thermal properties. The thermal stabilities (TGA and DTG) of the samples were analysed and are shown in Fig. 13a and b. Calcium alginate exhibited three stages of thermal decomposition; dehydration at 82–155 °C in the first stage, loss of the abundant hydroxyl groups on the calcium alginate at 220–300 °C in the second stage at a maximum temperature of 280 °C, and calcium carbonate decomposition at 628–800 °C in the final stage.

Plain paper without alginate fibres exhibited two-step decomposition between 50 and 100 °C due to dehydration and decomposition of the chemical structure of cellulose (glycosidic bonds) starting at 250 °C.

The composite paper containing calcium alginate fibres exhibited notable differences compared to the original paper. KA25 showed a small peak at 621 °C, whereas CA25 showed a peak at 710 °C, indicating calcium carbonate decomposition. On the other hand, KA50 and KA75 showed a more pronounced peak at 625 °C, while CA50 and CA75 showed a peak indicating the decomposition of calcium carbonate at 715 °C.[39] It is because calcium alginate is a substance that is naturally flame-retardant, and it produces inorganic particles while it burns, and the inorganic particles could act as a barrier or insulating the surface, slow down the production of combustible gases, and prevent further decomposition.[40] From these results, it can be seen that the composite with CA fibres added had a higher degradation temperature of calcium carbonate compared to KA fibres. This occurs because it might take more energy to break the bonds in the polymer chains in CA fibres than in KA fibres.

3.4.4. Inorganic particle formation. The thermal degradation of the calcium alginate fibres was found to vary with the temperature applied to the tube in the furnace at 200, 400, 600, and 800 °C and the residual ash was analysed by XRD to clarify the formation of inorganic particles at elevated temperatures, as shown in Fig. 14. Calcium alginate fibres from commercial alginate (CAF) did not show any significant peaks even when heated at 400 °C (CA400). The calcium alginate fibres from kelp alginate (KAF) exhibited peaks at = 27.3°, 29.4°, 32.3°, 45.5°, and 56.6° in 2θ, similarly to KA200. In the case of KA400, the XRD pattern of a $CaCO_3$ powder shows 2θ peaks at 23.1°, 29.4°, 36.0°, 39.5°, and 43.3°,[41] indicating that calcium carbonate started to form in CA600 with two small peaks that appeared at 28.1° and 38.4°, representing the formation of $Ca(OH)_2$ and CaO, respectively.[42] In the case of KA 600, two small peaks were also observed at 28.1° and 38.4°, indicating the formation of $Ca(OH)_2$ and CaO, respectively. In the CA800 sample, in total five additional peaks appeared at 18.0°, 47.0°, and 51.0° ($Ca(OH)_2$)[41] and at 32.3° and 55.7° (CaO). In the case of KA800, there were also additional peaks found as in CA800. The presence of $CaCO_3$ and CaO processed at high temperatures was exhibited by the XRD patterns of the calcium alginate fibres in the residual char. The presence of $CaCO_3$ in the composites efficiently increased the heat resistance

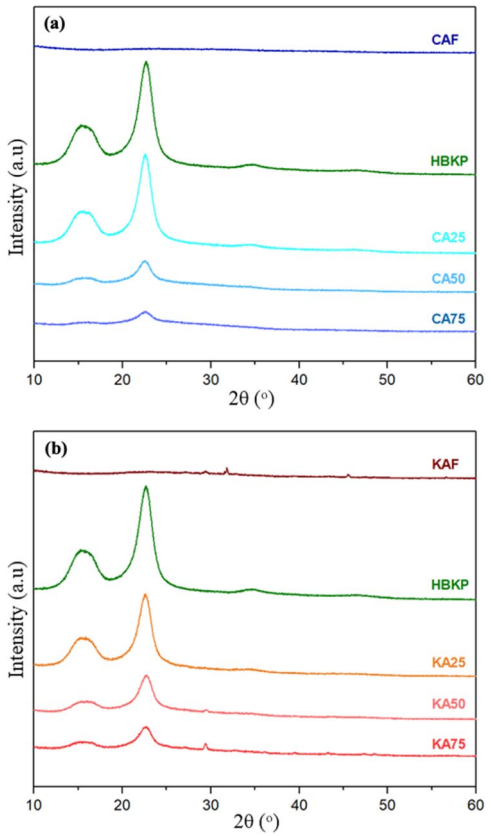

Fig. 15 XRD patterns of the calcium alginate fibres, HBKP, and paper composites containing (a) commercial alginate fibres (CA) and (b) kelp alginate fibres (KA).

of those materials, reduced mass loss, and enhanced their thermal stability and flame retardancy.[42]

Fig. 15 shows the XRD patterns of the calcium alginate fibres, paper, and paper composites. The main peaks of an HBKP sample that appeared at approx. 14.8° (1–10), 16.3° (110), and 22.6° (200) in 2θ are typical of cellulose I.[43] The crystallinity of the HBKP sheet was 95.4%. Both the calcium alginate fibre samples showed no significant crystal peak, indicating that calcium alginate fibre is an amorphous material.[44]

The crystallinities of the composite samples were 90.5%, 63.3%, 18.0%, 84.8%, 73.0%, and 62.2% for CA25, CA50, CA75, KA25, KA50, and KA75, respectively. When the composite was formulated with calcium alginate fibres, the XRD pattern of the paper composite showed a decrease in crystallinity. This occurs because calcium alginate fibre is an amorphous substance. This was attributed to the influence of the nucleation process on the crystallinity of the composite polymers, as the amorphous calcium alginate fibres disrupted the orderly arrangement of the polymer chains.

3.4.5 Chemical composition. Chemical composition analysis was performed using XPS on calcium alginate fibres after heat treatment in a tube furnace at 200, 400, 600, and 800 °C. The results of the XPS full spectra are shown in Fig. 16a and b, with three corresponding peaks, C_{1s} (approximately 287 eV), O_{1s} (approximately. 534 eV), and Ca_{2p} (approximately 350 eV), along with their relative atomic composition ratios. The C_{1s} spectrum of CAF and KAF in Fig. 16c and d indicates four groups, including –C–O–C– (286.5 eV),[45] –C–O– (287.3 eV),[34,46] –C(=O)– (288.5 eV),[45] and –COOH (290.5 eV),[34] respectively. These structures are derived from the macromolecular chains of cellulose and alginates. After heat treatment at 200, 400, 600,

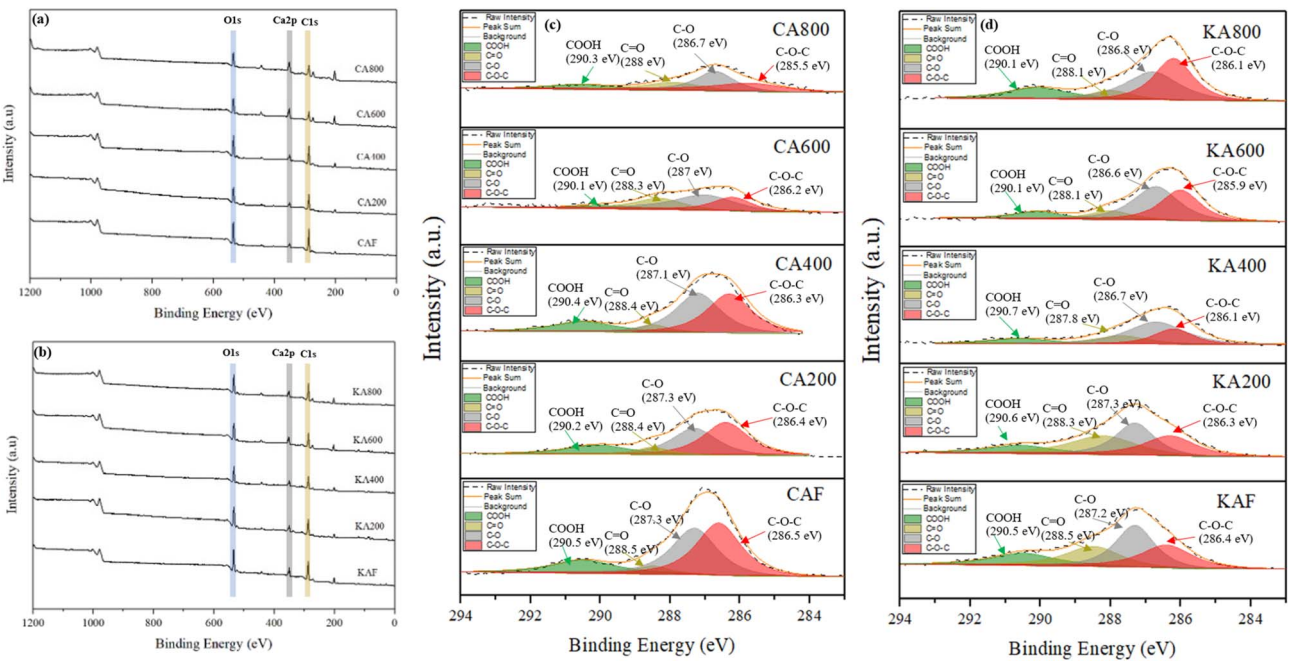

Fig. 16 XPS spectra of residual calcium alginate after thermal treatment at 200, 400, 600, and 800 °C in the wide scan of (a) the commercial alginate fibre sample and (b) the kelp alginate fibre sample, and high-resolution C_{1s} spectra of (c) commercial alginate fibres and (d) kelp alginate fibres.

and 800 °C for the CA and KA samples, no notable changes were observed in the C_{1s} peak.

In contrast, Tao *et al.*[38] showed an additional peak at 292.8 eV after burning, which is probably attributed to the $CaCO_3$ in the char residues and the peak at 295.9 eV was assigned to CaO. The $CaCO_3$ and CaO peaks should appear when heating at 600 °C in the CA600 sample and approximately 400 °C in the KA400 sample because the intensity of some peaks decreased. The physical barrier formed by $CaCO_3$ and CaO during combustion can be applied to the surface of fabrics to maintain heating and combustible gases while safeguarding the underlying fibres.[38]

4 Conclusions

We successfully extracted sodium alginate from *L. japonica* and *S. polycystum*. FTIR results were used to confirm that alginate produced using our extraction method has the same chemical structure as commercial alginate. Then, a sodium alginate solution was applied to form alginate fibres and a paper composite mixed with pulp fibres.

The results of tensile index analysis revealed that the paper composites containing 50% calcium alginate fibres had a better tensile index than other paper composite ratios; however, all composite samples still showed a lower tensile index than the pure HBKP (without the addition of the calcium alginate fibres). Thermal degradation analysis revealed an enhancement in the thermal stability of the composite papers compared to pure HBKP pulp. The XRD of the char residue confirmed the presence of $CaCO_3$, $Ca(OH)_2$, and CaO in char residues. These residues improved heat resistance, reduced mass loss, and enhanced both thermal stability and flame retardancy.

This study successfully produced composite paper from a blend of calcium alginate and wood pulp fibres. The findings suggest that calcium alginate fibres have potential for applications such as important documents, food packaging, domestic furnishings like padding, interior fittings such as thermal and sound insulation for walls, wallpaper decoration, structural coatings for wooden beams, and shipping and transportation materials.

Data availability

The datasets generated for this study are available on request from the corresponding author.

Author contributions

RM. M. N. F. performed most of the experiments and wrote the manuscript. K. T. performed some experimental work and guided the experiments. A. N. and M. K. guided and assisted the experiments. T. E. supervised the study and revised the manuscript accordingly. All authors have given their final approval for the publication of this manuscript.

Conflicts of interest

There are no conflicts to declare.

Acknowledgements

This research was partially supported by Science and Technology Research Partnership for Sustainable Development (SATREPS), Japan Science and Technology Agency (JST, JPMJSA2307)/Japan International Cooperation Agency (JICA). K. T. acknowledges the Ministry of Education, Culture, Sports, Science, and Technology (MEXT) of Japan for providing a scholarship under the Trans-World Professional Human Resources Development Program on Food Security & Natural Resources Management (TPHRD) for the Doctoral Course. We would like to thank the Open Facility Centre at the University of Tsukuba for allowing us to use their facilities and funding from the operating budget of the University of Tsukuba.

References

1 B. Carney Almroth and H. Eggert, *Rev. Environ. Econ. Pol.*, 2019, **13**, 317–326.
2 M. J. Fabra, M. Martínez-Sanz, L. G. Gómez-Mascaraque, J. M. Coll-Marqués, J. C. Martínez and A. López-Rubio, *Algal Res.*, 2017, **28**, 80–87.
3 C. Mathiot, P. Ponge, B. Gallard, J.-F. Sassi, F. Delrue and N. Le Moigne, *Carbohydr. Polym.*, 2019, **208**, 142–151.
4 J. Venkatesan, S. Anil, S.-K. Kim and M. S. Shim, *Polymers*, 2016, **8**, 30.
5 M. Fertah, in *Seaweed Polysaccharides*, ed. J. Venkatesan, S. Anil and S.-K. Kim, Elsevier, 2017, pp. 11–26.
6 I. Donati, Y. A. Mørch, B. L. Strand, G. Skjåk-Bræk and S. Paoletti, *J. Phys. Chem. B*, 2009, **113**, 12916–12922.
7 I. I. Kabir, C. C. Sorrel, S. S. Morafah, W. Yang, A. C. Y. Yuen, M. T. Nazir and G. H. Yeoh, *Polym. Rev.*, 2021, **61**, 357–414.
8 M. Zhang and X. Zhao, *Int. J. Biol. Macromol.*, 2020, **162**, 1414–1428.
9 F. Fahma, R. M. Fauzan, T. Sunarti, S. Sugiarto, A. Halim, K.-H. Lin, D. Hu and T. Enomae, *J. Nanostruct.*, 2020, **10**, 779–792.
10 X. Fan, R. C. Domszy, N. Hu, A. J. Yang, J. Yang and A. E. David, *J. Sol-Gel Sci. Technol.*, 2019, **91**, 11–20.
11 Y. Kobayashi, R. Matsuo and H. Kawakatsú, *J. Appl. Polym. Sci.*, 1986, **31**, 1735–1747.
12 Y. Qin, *Polym. Int.*, 2008, **57**, 171–180.
13 Y. Salosso, *AACL Bioflux*, 2019, **12**, 2130–2136.
14 P. Kaladharan, *Kadalekum Kanivukal (Bounties of the Sea)*, 1998, pp. 76–79.
15 H. Andriamanantoanina and M. Rinaudo, *Carbohydr. Polym.*, 2010, **82**, 555–560.
16 L. A. Bashford, R. S. Thomas and F. N. Woodward, *J. Soc. Chem. Ind.*, 1950, **69**, 337–343.
17 D. J. McHugh, Production and Utilization of Products from Commercial Seaweeds, *FAO Fish. Tech. Pap.*, 1987, **288**, 58–115.

18 S. Saji, A. Hebden, P. Goswami and C. Du, *Sustainability*, 2022, **14**, 5181.
19 A. Dodero, S. Alberti, G. Gaggero, M. Ferretti, R. Botter, S. Vicini and M. Castellano, *Adv. Mater. Interfaces*, 2021, **8**, 2100809.
20 R. Ahmad Raus, W. M. F. Wan Nawawi and R. R. Nasaruddin, *Asian J. Pharm. Sci.*, 2021, **16**, 280–306.
21 C. G. Gomez, M. V. Perez Lambrecht, J. E. Lozano, M. Rinaudo and M. A. Villar, *Int. J. Biol. Macromol.*, 2009, **44**, 365–371.
22 M. R. Torres, A. P. Soursa, E. A. Silva Filho, D. F. Melo, J. P. Feitosa, R. C. de Paula and M. G. Lima, *Carbohydr. Res.*, 2007, **342**, 2067–2074.
23 F. Clementi, M. Mancini and M. Moresi, *J. Food Eng.*, 1998, **36**, 51–62.
24 A. V. Skriptsova, N. M. Shevchenko, D. V. Tarbeeva and T. N. Zvyagintseva, *Mar. Biotechnol.*, 2012, **14**, 304–311.
25 A. Mohammed, A. Rivers, D. C. Stuckey and K. Ward, *Carbohydr. Polym.*, 2020, **245**, 116419.
26 G. Y. Kim, Y. H. Seo, I. Kim and J. I. Han, *Sci. Total Environ.*, 2019, **673**, 750–755.
27 X. Xu, J. Y. Kim, Y. R. Oh and J. M. Park, *Bioresour. Technol.*, 2014, **169**, 455–461.
28 S. Istini, M. Ohno and H. Kusunose, *Bulletin of Marine Science and Fisheries*, 1994, **14**, 49–55.
29 S. L. LIM, S. H. S. Khalafu, W. A. W. Mustapha and S. J. Lim, *Sains Malays.*, 2017, **46**, 1807–1816.
30 C. Yamashita, I. C. Freitas Moraes, A. G. Ferreira, C. C. Zanini Branco and I. G. Branco, *Carbohydr. Polym.*, 2021, **251**, 116992.
31 H. d. S. Costa and M. R. Dias, *Mater. Res.*, 2021, **24**, DOI: 10.1590/1980-5373-MR-2020-0587.
32 N. J. Borazjani, M. Tabarsa, S. You and M. Rezaei, *Int. J. Biol. Macromol.*, 2017, **101**, 703–711.
33 W.-P. Voo, B.-B. Lee, A. Idris, A. Islam, B.-T. Tey and E.-S. Chan, *RSC Adv.*, 2015, **5**, 36687–36695.
34 A. Jejurikar, X. T. Seow, G. Lawrie, D. Martin, A. Jayakrishnan and L. Grøndahl, *J. Mater. Chem.*, 2012, **22**, 9751–9758.
35 L. Montes, M. Gisbert, I. Hinojosa, J. Sineiro and R. Moreira, *Carbohydr. Polym.*, 2021, **272**, 118455.
36 F. Wang and J. Shao, *Polymers*, 2014, **6**, 3005–3018.
37 H. Kakita and H. Kamishima, in *Nineteenth International Seaweed Symposium: Proceedings of the 19th International Seaweed Symposium, Held in Kobe, Japan, 26–31 March, 2007*, ed. M. A. Borowitzka, A. T. Critchley, S. Kraan, A. Peters, K. Sjøtun and M. Notoya, Springer Netherlands, Dordrecht, 2009, pp. 93–99, DOI: 10.1007/978-1-4020-9619-8_13.
38 Y. Tao, B. Wang, C. Liu, P. Li, Y.-J. Xu, Z.-M. Jiang, Y. Liu and P. Zhu, *Cellulose*, 2021, **28**, 4495–4510.
39 Q.-s. Kong, B.-b. Wang, Q. Ji, Y.-z. Xia, Z.-x. Guo and J. Yu, *Chin. J. Polym. Sci.*, 2009, **27**, 807–812.
40 J. Zhang, Q. Ji, X. Shen, Y. Xia, L. Tan and Q. Kong, *Polym. Degrad. Stab.*, 2011, **96**, 936–942.
41 W. Gu, D. W. Bousfield and C. P. Tripp, *J. Mater. Chem.*, 2006, **16**, 3312–3317.
42 J. Li, Z. Li, X. Zhao, Y. Deng, Y. Xue and Q. Li, *J. Therm. Anal. Calorim.*, 2018, **131**, 2167–2177.
43 G. H. D. Tonoli, L. E. Silva, D. Wood, L. Torres, T. Williams, J. E. Oliveira, A. S. Fonseca, A. Klamczynski, G. Glenn and W. Orts, *Cerne*, 2021, **27**, e–102647.
44 G. Wang, X. Wang and L. Huang, *Biotechnol. Biotechnol. Equip.*, 2017, **31**, 766–773.
45 S. Fuxiang, W. Na, Z. Qiangqiang, W. Jie and L. Bin, *J. Hazard. Mater.*, 2022, **440**, 129774.
46 J. Yu, J. Wang and Y. Jiang, *Nucl. Eng. Technol.*, 2017, **49**, 534–540.